

Autonomous Sailboat Navigation for Short Course Racing

Roland Stelzer ^{a,b,*} and Tobias Pröll ^b

^a*De Montfort University, Centre for Computational Intelligence
The Gateway, GB - Leicester LE1 9BH, United Kingdom.*

^b*Austrian Association for Innovative Computer Science
Kampstraße 15/1, A-1200 Vienna, Austria.*

Abstract

The paper presents a compact method to calculate a suitable route for a sailboat in order to reach any specified target. The calculation is based on the optimisation of the time-derivative of the distance between boat and target and features a hysteresis condition, which is of particular importance for beating to windward. The algorithm provides an answer to the perennial question when to tack on upwind courses. Further, it immediately adapts to varying wind conditions. The resulting routes for different conditions are analysed on the basis of a simulation featuring a mathematical boat model. Experiments have been carried out using an unmanned and autonomously controlled sail boat. The navigated route agrees well with the simulation results.

Key words: Autonomous Sailing, Route Optimisation, Sailboat Navigation, Optimum Beating, Leeway Drift Compensation

* Corresponding author. Address: Kampstraße 15/1, A-1200 Vienna, Austria.

Email addresses: rstelzer@dmu.ac.uk, roland.stelzer@innoc.at (Roland Stelzer), tobias.proell@innoc.at (Tobias Pröll).

URLs: <http://www.cci.dmu.ac.uk>, <http://www.innoc.at> (Roland Stelzer), <http://www.innoc.at> (Tobias Pröll).

Nomenclature

Roman Symbols

a_k	coefficient for polynomial polar diagram in Equation 9 in deg^{-k}
B	boat position in m
f_d	leeway factor in Equation 7
f_{polar}	function referring to Equation 3 in Figure 6 in $m \cdot s^{-1}$
k	counter in 9
LAT	geographic latitude
LON	geographic longitude
n	hysteresis factor
\vec{n}_0	normal unit vector on boat heading
p_c	beating parameter in m
R_e	average Earth's radius in m
\vec{t}	vector boat to target in m
T	target position in m
\vec{v}_b	boat speed vector in $m \cdot s^{-1}$
\vec{v}'_b	boat speed vector for alternative heading in $m \cdot s^{-1}$
\vec{v}_d	lateral speed vector due to leeway in $m \cdot s^{-1}$
v_t	velocity made good
v'_t	velocity made good for alternative heading
\vec{w}	wind speed vector in $m \cdot s^{-1}$

Greek Symbols

α	true wind angle relative to boat heading according to Equation 7
φ	angle, in general

Subscripts

0	indicating vector of unit length
<i>abs</i>	referring to true wind (absolute wind)
<i>b</i>	referring to the boat
<i>d</i>	referring to leeway drift
<i>hyp</i>	hypothetical velocity during optimization loop in Figure 6
<i>inv</i>	inverse direction or vector respectively
<i>L</i>	left hand side referring to true wind direction
<i>max</i>	referring to maximum target efficiency reached
<i>new</i>	new boat heading as the result of the algorithm in Figure 6
<i>R</i>	right hand side referring to true wind heading
<i>rel</i>	referring to apparent wind (relative wind)
<i>t</i>	referring to target
<i>tn</i>	referring to a certain point in time
<i>w</i>	referring to apparent wind (relative wind)

Acronyms

<i>FIS</i>	Fuzzy Inference System
<i>VMG</i>	Velocity Made Good

1 Introduction

For motorised vehicles in isotropic, stationary environments, where a straight line is the shortest way to a target both in terms of distance and time, the identification of an optimum heading to reach the target is trivial. This is significantly different for sailboats, where a straight line route to the target may not even be navigable if the target is located upwind - the sailor has to beat (sailing a zigzag course) in this case.

Ship routeing can be considered as the *“procedure where an optimum track is determined for a particular vessel on a particular run, based on expected weather, sea state and ocean currents”* [1]. Optimisation can be performed in terms of

- minimum passage time
- minimum fuel consumption
- safety for crew and ship
- best passenger comfort

or a combination of the criteria above [1,2]. The present work focuses on minimum passage time. Fuel consumption is obsolete for exclusively wind propelled vehicles. Safety issues go beyond the focus of this study. However, obstacle and thunderstorm avoidance are major tasks for future work. Passenger comfort can be obtained by appropriate control of sails and rudder dependent on the boat dynamics [3].

The existing approaches for long term weather routeing all require, more or less, certain weather predictions and a description of the boat’s behaviour under certain wind conditions determined by a boat specific polar diagram [4,5]. The polar diagram describes the maximum speed a particular sailboat can reach dependent on wind speed and direction.

Most common computerised weather routeing techniques are either an implementation of the manual isochrone plotting or optimisation methods within a discrete geographical grid system along the great circle route. Motte and Calvert illustrated the effect of incorporating various discrete grid systems in a weather routeing system, which employs Bellman’s dynamic programming algorithm [6]. Stawicki and Smierzchalski mentioned evolutionary algorithms as a promising approach to weather routeing [7]. Actual implementations of evolutionary path planning at sea have been published [8,9] but do not address the special situation of sailboats. All these approaches rely on weather forecast information on the one hand and sea charts on the other hand.

Philpott and Mason discuss two models to deal with uncertain weather data on short and long course routing [10]. They consider the possibility of different

weather conditions evolving in the future to determine routes which perform well under all of them.

The proposed approach in this research does not need a weather forecast at all. As the local wind conditions often change and accurate weather forecasts are not available for very short distances and periods, only local and present wind conditions are taken into account in order to determine an optimum heading for the vessel. The method reacts on changes of the wind conditions in real-time by recalculating the heading periodically.

Because the short-term weather is rather unpredictable the approach deals with locally measured weather only, similar to a human sailor on a short regatta.

In the following, a calculation strategy for suitable boat headings in order to reach a specific target point is presented, tested in simulations, and experimentally demonstrated using a fully autonomous sailboat. First, the boat behaviour is described and the basic principles of the routeing method are presented before reporting the flow chart of the algorithm. The particularities of the proposed strategy are illustrated by simulations using a computer model of a sailboat. Finally, the algorithm is tested on an unmanned autonomous sailboat equipped with an on-board computer system and necessary sensor and actuator devices.

2 Routeing Strategy

2.1 Local Coordinate System

For means of illustration and convenient use of vector operations, local Cartesian coordinates are used to describe the navigated water surface. The simplified assumption implies that the water surface is considered to be flat. This is a good approximation in most cases unless oceans are to be crossed. The point of origin of the local system is set somewhere close to the route, e.g. to the starting point or to a reference point nearby on shore. The transformation between the geographic position and the local system is defined as follows:

$$x = R_E \cdot \cos(LAT) \cdot \frac{\pi}{180 \text{ deg}} \cdot LON \quad (1)$$

$$y = R_E \cdot \frac{\pi}{180 \text{ deg}} \cdot LAT \quad (2)$$

This means that the x-axis always leads to the east while the y-axis leads to the north. The conventional way of drawing x,y-charts therefore results in the conventional view on northern hemisphere maps where north is towards the top and east is on the right hand side. It is important to notice that the transformation to Cartesian coordinates is done mostly for means of illustration. The navigation strategy can be formulated in a similar way for geographic coordinates using great circle routes, compass headings, and trigonometric functions instead of straight lines, normalized vectors, and vector analysis. According to the following description, the boat virtually moves on a flat water surface neglecting the Earth's curvature.

2.2 Sailboat Behaviour (Polar Diagram)

The actual speed a sail boat can reach in a certain direction depends on the wind speed but also on the angle between boat heading and wind direction: while no direct course is possible straight into the wind, the maximum speed is usually obtained with the wind from the rear side at about $\pm 120deg$. This dependency can be plotted continuously as the boat-specific polar diagram (Fig. 1).

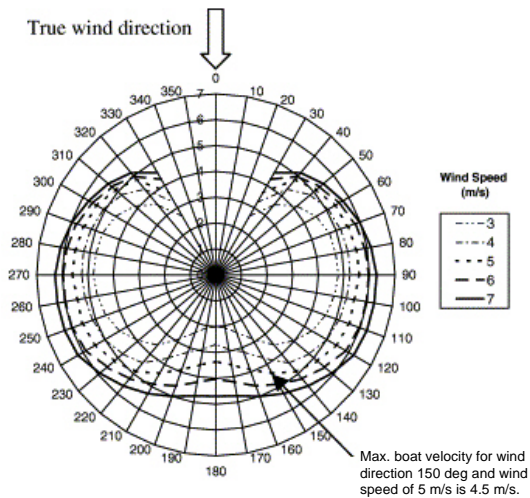


Fig. 1. Example of a Polar Diagram [11]

The boat speed is therefore given as a function of the wind speed and the angle between true wind and boat heading:

$$|\vec{v}_b| = f(|\vec{w}_{abs}|, |\varphi(\vec{v}_b) - \varphi(\vec{w}_{abs})|) \quad (3)$$

The polar speed diagram normally shows the norm of the boat velocity vector. Lateral forces caused by the wind lead to a leeway drift. The heading

of the boat is therefore always slightly closer towards the wind than the actual direction of movement. As leeway is a very important factor in sailboat route planning, the leeway drift behaviour of the sailboat needs to be considered. However, the diagram in Fig. 1 does not include information about the difference in directions of boat heading and actual movement. Additional information about leeway drift as a boat dependent function of wind speed and direction is required.

2.3 Quantification of Target-Approach (Velocity Made Good)

In order to get from a current position of the boat B to a target point T , both the direction of the target and the wind must be considered. The aim of the routing algorithm is therefore to decrease the distance to the target as fast as possible. The efficiency of a certain boat heading in approaching the target can be directly quantified projecting the boat speed vector on the target direction:

$$v_t = \vec{v}_b \cdot \vec{t}_0 \quad (4)$$

Eq. (4) is illustrated in Fig. 2(a). The boat speed vector \vec{v}_b can be considered to be a function of the boat heading $\vec{v}_{b,0}$ and the wind vector according to Eq. (3). If the target is located in the direction the wind comes from, the optimal route is a compromise between aiming towards the target and getting speed. The goal for the routing algorithm is to identify the boat heading for which the velocity made good v_t , which represents the negative time-derivative of the distance between boat and target, is maximised. The same approach works if the target is located in any direction relative to the wind direction (Figs. 2(b), 2(c)). However, the optimal boat heading indicated by the direction of the speed vector changes as the boat moves on its trajectory. The situation in Fig. 2(b) promises unique identifiers for the optimum boat heading until the target is reached and the steady correction of the boat heading is smooth along the trajectory. The situations in Figs. 2(a) and 2(c), however, will lead to constellations where there are two headings of equal maximum velocity made good to follow, one on the right and one on the left hand side of the wind direction. This happens when the target direction aligns with the wind direction (Fig. 3). In order to get a unique proposal for the heading to follow, a hysteresis condition is applied.

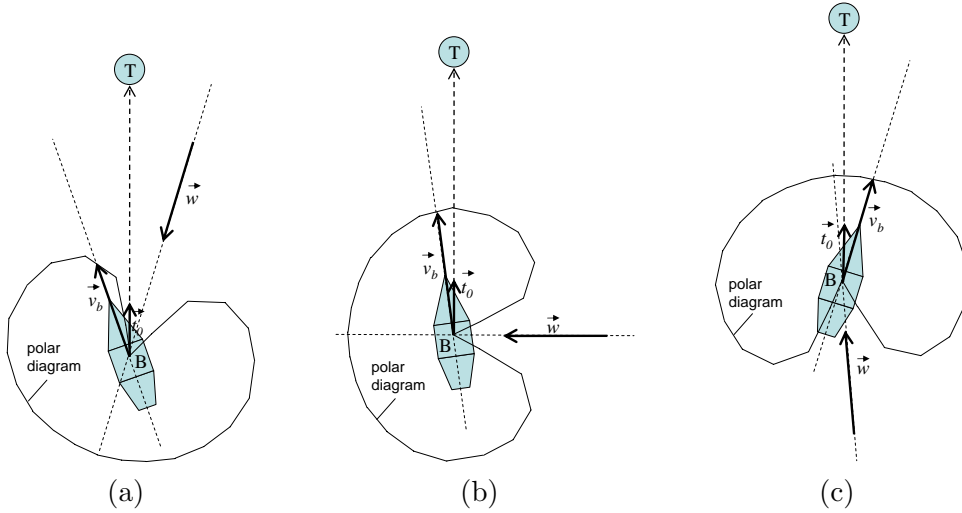


Fig. 2. Possible Constellations and Definition of Velocity Made Good

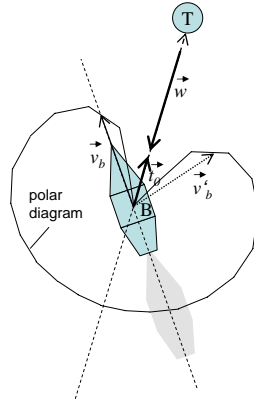


Fig. 3. Two Global Optima for Target Efficiency

2.4 Beating Hysteresis and Beating Parameter

In practice, the sailor beats about if the target is within the angle where no direct navigation is possible. In the terms of our analytical approach, this means that the boat follows a local optimum \vec{v}_b (close to the recent heading) for a certain time until the global optimum \vec{v}'_b is significantly better than \vec{v}_b . At this point, the boat turns for the global optimum \vec{v}'_b , which will be followed until an alternative heading is significantly better leading to the next turn and so on. Beating is illustrated in 4, the hysteresis factor n is defined by:

$$v'_t > n \cdot v_t \rightarrow \text{turn for } \vec{v}'_b; n > 1 \quad (5)$$

In order to obtain a reasonable behaviour of the algorithm, n must be larger than one. It can be shown that a constant hysteresis factor leads to a sector-shaped beating area with an increasing frequency of turns in the vicinity of the target. In order to obtain a more or less rectangular beating area of defined

width, the hysteresis parameter n is expressed as a function of the distance to the target as follows:

$$n = 1 + \frac{p_c}{|t|} \quad (6)$$

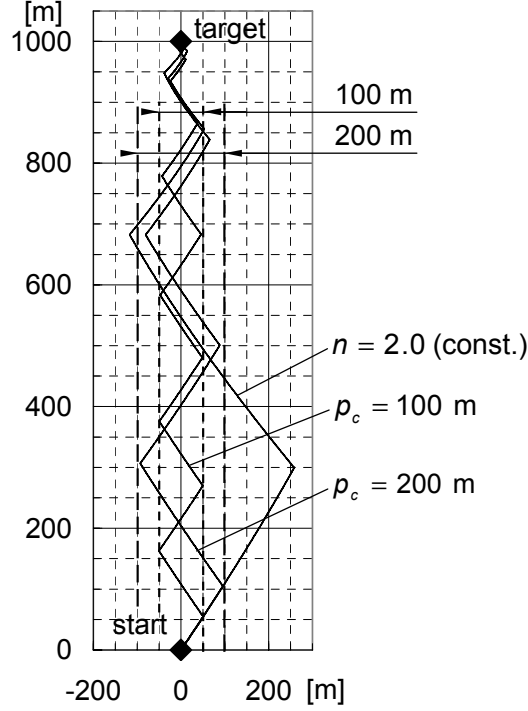


Fig. 4. Effect of Hysteresis Factor on Beating Area

The constant beating parameter p_c in Eq. (6) has the dimension of a length and is proportional to the width of the rectangular beating band in adequate distance from the target. For the polar diagram chosen for generation of Fig. 4, the width of the beating band coincides with value of the beating parameter (proportionality factor of one). Of course, the orientation of this rectangular beating area can change as the wind direction may change in time. It is important to note that the beating hysteresis can be globally applied and works without adaptation also in the case where the target is in the direction towards which the wind blows (Fig. 2(c)). The time-losses of manoeuvres are not considered in the conditions for tacking (Eq. (5) and Eq. (6)). For a reasonable width of the beating band, however, these losses are negligible.

Simulation shows that all three courses in Fig. 4 need the same time to reach the target if manoeuvre costs are not considered. This is plausible because the mean boat heading against the wind is constant regardless of the beating band width. Optimisation with respect to manoeuvre losses would always lead to a course with only one tack. However, a route with only one tack requires a lot of lateral space and is less flexible regarding spontaneous changes

of the wind direction. Theoretically, if manoeuvre losses are neglected, the overall route performance does not depend on the beating band width. The beating parameter should therefore be chosen as a compromise between the available, obstacle free area and a reasonable number of tacks considering possible changes of wind direction.

2.5 Leeway Drift Consideration

If the boat is steered in the direction proposed by the optimisation of velocity made good (optimum boat heading), the boat will actually move into a slightly different direction due to leeway drift. The goal of the optimisation procedure, however, is to make the boat move a certain optimum direction rather than to specify the boat heading. To account for leeway drift, the lateral speed component is estimated as a function of the wind vector:

$$\vec{v}_d = f_d \cdot \vec{n}_{b,0} \cdot (\vec{n}_{b,0} \cdot \vec{w}_{abs}) \quad (7)$$

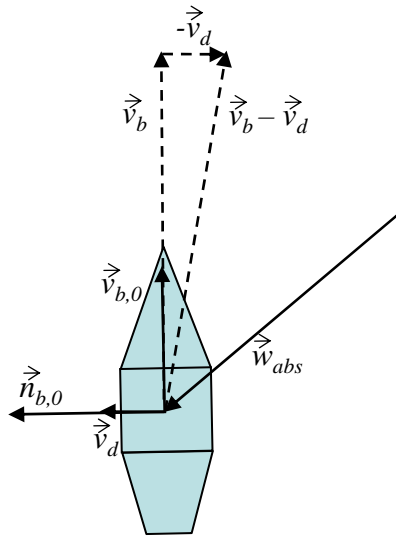


Fig. 5. Leeway Model

The leeway velocity \vec{v}_d is added to the calculated boat speed vector from the boat polar diagram. The dimensionless leeway factor f_d depends on the boat and can be experimentally determined. The boat heading has to be adjusted to $\vec{v}_b - \vec{v}_d$ in order to achieve the boat movement in the optimum direction \vec{v} .

2.6 Summary of Algorithm and Implementation

The data needed to decide for the boat heading in order to efficiently reach the target are:

- target position T
- current boat position B
- current boat heading $\varphi(\vec{v}_b)$
- true wind direction and speed (i.e. wind vector \vec{w}_{abs})

The current boat heading is needed in order to decide whether a proposed direction requires a tack or not. The wind speed is only needed if the polar diagram shows a significantly nonlinear dependency on the wind speed. Otherwise, only the direction of the true wind is actually required and a normalised polar diagram is used. At this point we assume that the necessary data are available. The practical determination of the true wind from different sensor values will be treated in the experimental section below.

The presented routing algorithm generally assumes that

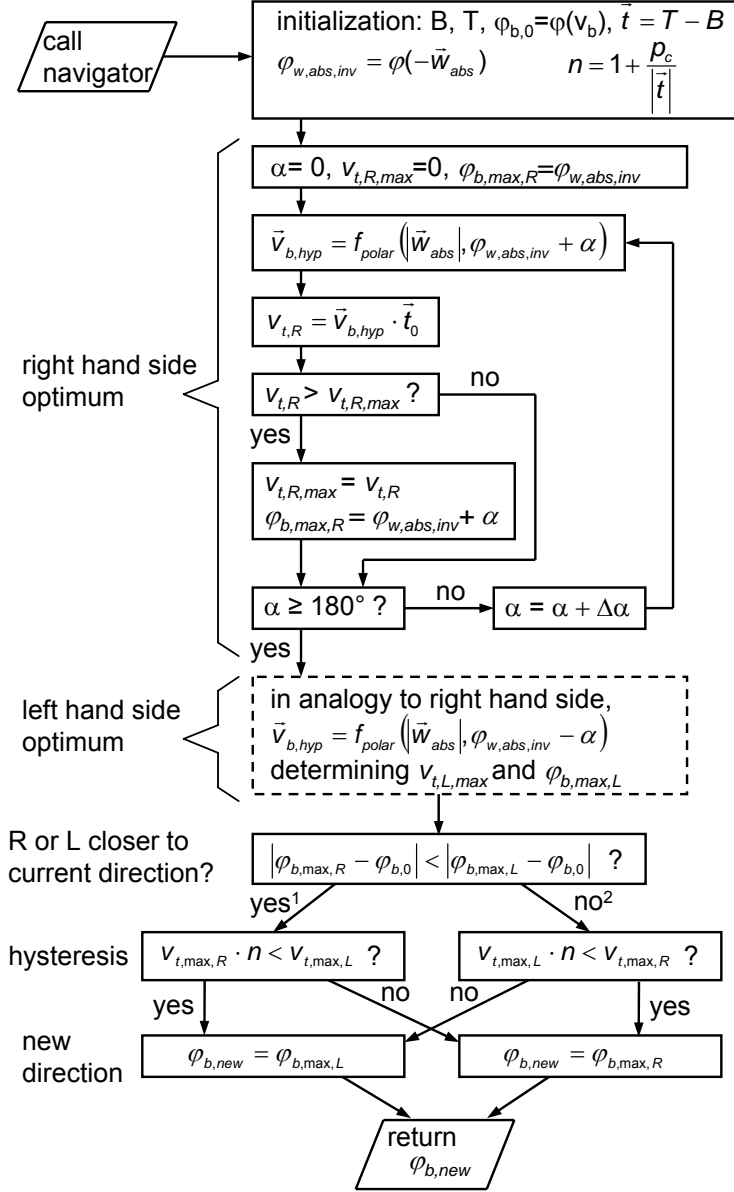
- the true wind is the same all over the area between boat and target and
- the true wind will remain for the whole leg as it is in the moment (or as it has been over a recent time interval for average wind determination respectively)

The first assumption is reasonable for small to medium range environments like lakes or coastal regions and the second assumption reflects the knowledge of a sailor without consideration of the weather forecast.

The overall structure of the routing algorithm is illustrated in Fig. 6. The aim is the calculation of a suitable boat heading in the form of an angle (which can subsequently be transformed to a unit vector) for a given parameter set. The routing algorithm is called again and again in reasonable time steps in order to update the proposed heading as the surrounding parameters change. This applies especially for the target direction as a result of boat movement.

3 Experimental Setup

Experiments on the routing algorithm were carried out on a computer simulation first, and afterwards on the 1.38 m yacht model *Roboat I* based on the boat type “Robbe Atlantis” (Fig. 7) under real-world conditions. The boat won in the first Microtransat competition for autonomous sailboats in June 2006 in Toulouse, France. The event was organised by Ecole Nationale Supérieure d’Ingénieurs de Constructions Aéronautiques (ENSICA) in Toulouse. The ambitious aim was to demonstrate completely autonomous sailing, where routing, navigation and carrying out the manoeuvres have to run automatically directly on the boat.



- 1) right hand side optimum closer to current boat direction
 2) left hand side optimum closer to current boat direction

Fig. 6. Structure of the Short Course Routing Algorithm

The *Robot I* is usually used as a remote controlled sailboat. For our purposes, the boat is additionally equipped with various sensors to measure the environmental conditions. A computer program called “abstractor” running on the boat gathers sensor data and transforms them into semantically useful information for the routing software.

Fig. 8 shows the relationship between measured sensor data and prepared information. The target position T is statically defined for a particular leg and needs not to be measured. The current boat position B is measured by

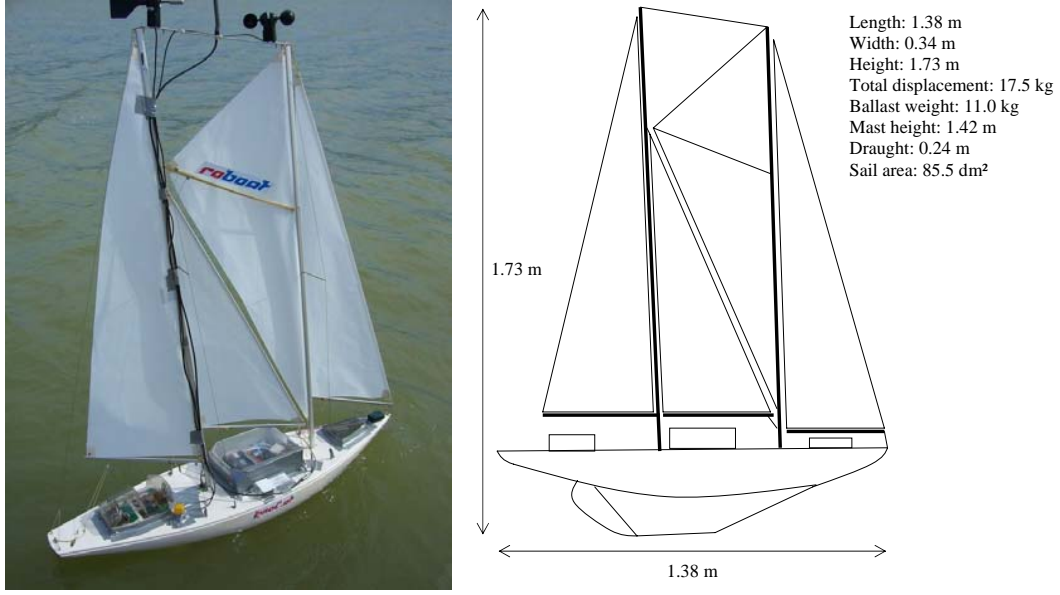


Fig. 7. Roboat I

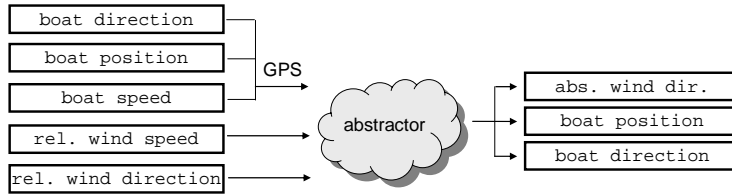


Fig. 8. Sensor Data Processing

a GPS receiver. The “abstractor” transforms the GPS coordinates into the metric Cartesian coordinate system. A tilt compensated compass delivers the boat heading $\varphi(\vec{v}_b)$. Because of inaccuracy of the sensor data some damping is applied. The true wind \vec{w}_{abs} has to be calculated out of the apparent wind \vec{w}_{rel} and the boat velocity \vec{v}_b (Eq. (8) and Fig. 9), where \vec{v}_b is a combination of $\varphi(\vec{v}_b)$ and actual boat speed $|\vec{v}_b|$ measured by the GPS receiver.

$$\vec{w}_{abs} = \vec{w}_{rel} + \vec{v}_b \quad (8)$$

4 Results and Discussion

Since the shapes of the curves for varying wind speed are largely concentric (Fig. 1), a normalised shape-function multiplied with the true wind speed is used to describe the polar diagram of the boat for the present work. The coefficients $a_0 \dots a_5$ in Eq. (9) for α in deg are listed in Table 1 and the resulting

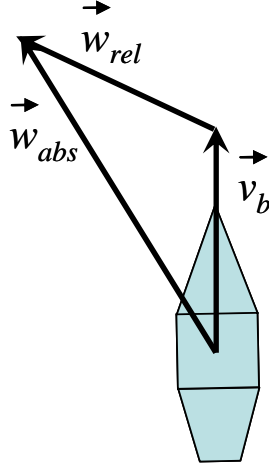


Fig. 9. True and Apparent Wind

graph is shown in Fig. 10.

$$|\vec{v}_b| = \max \left(0, |\vec{w}_{abs}| \cdot \sum_{k=0}^5 (a_k \cdot a^k) \right) \quad (9)$$

Coefficient	Value	Unit
a_0	-1.3956	-
a_1	$1.0786 \cdot 10^{-1}$	deg^{-1}
a_2	$-2.3250 \cdot 10^{-3}$	deg^{-2}
a_3	$2.4255 \cdot 10^{-5}$	deg^{-3}
a_4	$-1.1939 \cdot 10^{-7}$	deg^{-4}
a_5	$2.2054 \cdot 10^{-10}$	deg^{-5}

Table 1

Coefficients for the Normalised Polar Diagram (According to Eq. (9))

The polar diagram according to Fig. 10 is used to describe the boat behaviour in the following computer simulations. The routing algorithm uses either this polar diagram or a binary simplification returning a constant average speed for courses between 43 and 151 deg (broken line in Fig. 10). The boundaries of the simple polar diagram have been chosen based on time-optimum simulation results. It is important to notice that the consideration of leeway drift in the routing algorithm leads to boat headings closer to the wind than the proposed optimal course. The closest proposed direction of boat movement against the wind is predefined by the shape of the polar diagram used in the routing algorithm. To avoid getting stall against the wind, these closest courses must keep room within the navigable range for heading adjustment due to leeway drift compensation. This requirement has a direct impact on the shape of an

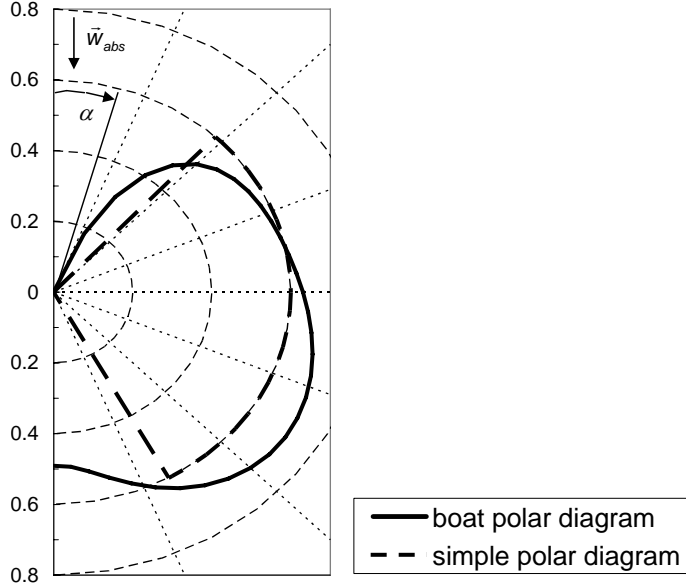


Fig. 10. Normalised Polar Diagram Used Within the Present Work (According to Eq. (9) and Table 1 for Unit Wind Speed)

efficient polar diagram, which can, as it will be shown below, differ from the actual boat polar diagram.

For a simple course connecting two points, the routes proposed by the routing algorithm are shown in Fig. 11 for different constant wind conditions. The beating parameter is set to $60\ m$ for all runs. The mathematical model of the boat behaves strictly according to the boat polar diagram without consideration of leeway. In each case, the use of either the boat polar diagram or the simple polar diagram for the routing algorithm is compared.

If the target is located upwind (Fig. 11(a)), the proposed routes are almost the same for both cases. The boat must tack several times and the approximately constant width of the beating band can be observed in the illustration. In the situations where the wind blows laterally within the navigable range (Figs. 11(b) to 11(d)), a straight line route is supported by the algorithm featuring the simple polar diagram while the consideration of the boat polar diagram leads to deviations from the straight line. The reason for this behaviour is that higher target efficiencies can be reached according to the boat polar diagram if the boat heading deviates from the straight line. However, this optimisation is only true for the very moment and does not consider possible disadvantages later in the course. In Fig. 11(e), where the wind blows straight towards the target, three possible routes are compared. The algorithm suggests routes where the boat gybes several times for both polar diagrams (boat and simple). The third possibility considered in Fig. 11(e) is the straight line.

In order to quantitatively compare the different routes in Fig. 11, the reciprocal target approaching velocity (reciprocal value of velocity made good) is plotted

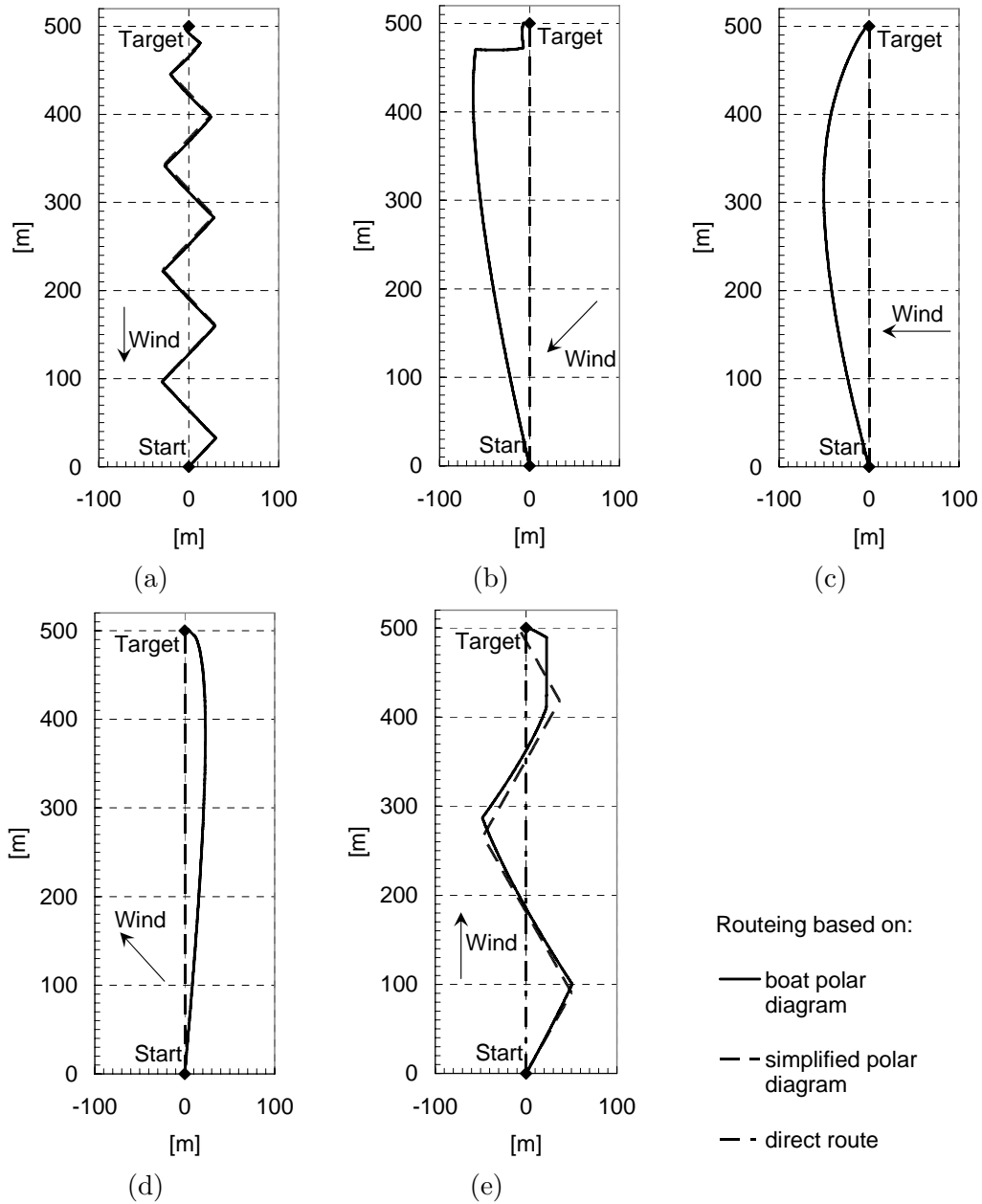


Fig. 11. Routing Simulation Results for Different Constant Wind Directions

versus the distance to the target in Fig. 12. In these diagrams, the area below the graphs corresponds to the time needed to reach the target (time effort). The time efforts of the different routes are summarised in Table 2.

The proposed routes do not significantly differ for the case where the target is located upwind (Fig. 12(a)). If the wind is blowing laterally, it turns out that the straight line route proposed by application of the simple polar diagram in the routing algorithm is advantageous at least for the wind directions investigated. Figs. 12(b) to 12(d) show the time effort in the case that the direct route is most efficient. This seems to be paradoxical at first sight because

the use of the actual boat polar diagram in the routeing algorithm always follows the direction of highest velocity made good. However, the boat takes a longer route and manoeuvres into areas where the target cannot be approached efficiently any more.

Fig. 13 illustrates how the application of the boat polar diagram leads to such a non-optimal route. The diamonds in Fig. 13 show the position of the boat in certain points in time on the straight line route (B_{tn}) and on sub-optimal route based on the boat polar diagram (B'_{tn}). In the very beginning, the proposed non-direct route allows a higher velocity made good. After time step 6, the direct route is already closer to the target than the route with local optimisation of velocity made good. In addition, the boat position of the non direct route at time step 6 is such that the target is in an unfavourable direction with respect to the wind.

For the case where the target is straight in the wind direction (Fig. 12(e)) the proposed routes are both better than the straight line route. The reason is the characteristic shape of the boat polar diagram, where the maximum speed is reached at angles between 120 and 140 *deg* from the direction the wind blows from (broad reach course).

Time Effort in <i>s</i>	Wind Direction in <i>deg</i>				
	(0 <i>deg</i> in Positive x-Direction)				
	270	225	180	135	90
Boat Polar Diagram	2850	2175	1680	1510	1930
Simple Polar Diagram	2835	2010	1630	1460	1860
Straight Line Route	<i>Not possible</i>	2010	1630	1460	2095

Table 2
Time Effort for the Routes Discussed in Figs. 11 and 12 (Polar Diagram According to Table 1 and Unit Wind Speed)

Summarising, the simulation shows that the routeing algorithm does not require the knowledge of the detailed boat speed polar diagram in order to propose suitable routes. Moreover, the routes proposed by application of the simplified polar diagram from Fig. 10 are even more time-effective than those proposed on the basis of the boat polar diagram. The time-effort of a certain route between two points can be illustrated according to Fig. 12.

The simulation above assumes that the boat behaves strictly according to the boat polar diagram. In order to prove the practical applicability of the proposed routeing algorithm, test runs have been carried out using the demonstration sail boat *Roboat I*. It is important to notice that the exact polar speed diagram of the demonstration boat is not known and secondary effects like lee-

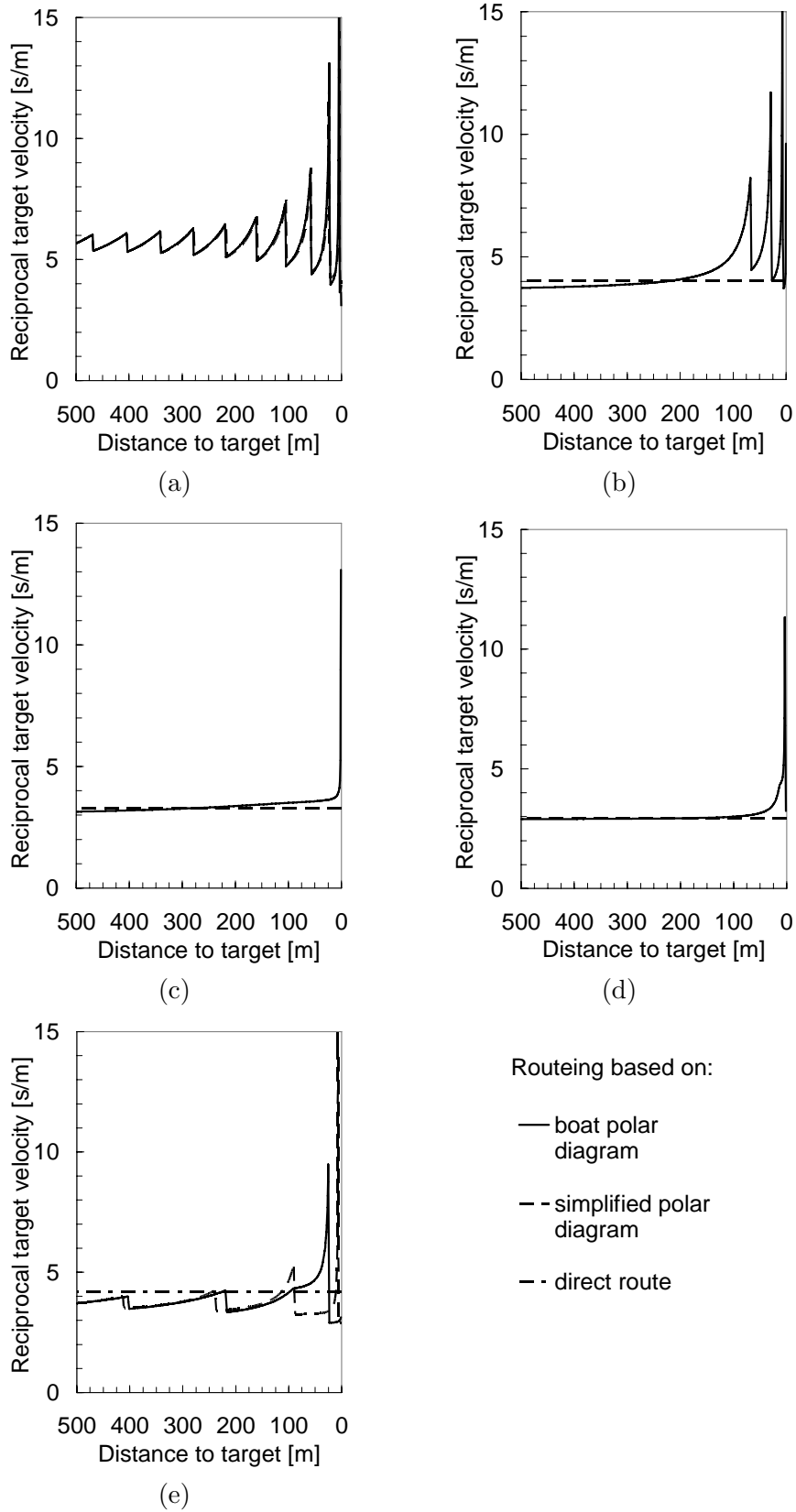


Fig. 12. Efficiency Comparison for the Different Routes Shown in Fig. 11

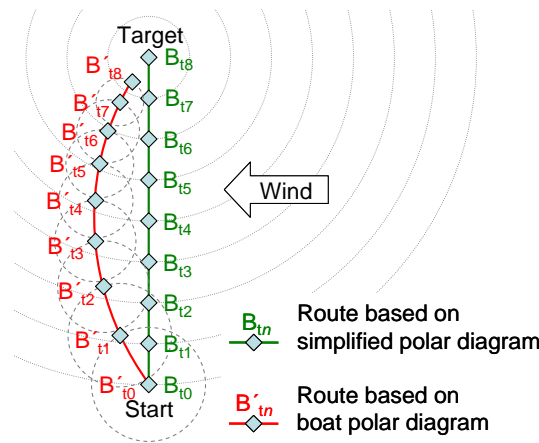


Fig. 13. Illustration of Efficiency Comparison on Beam Reach Course (Situation as in Figs. 11(c) and 12(c))

way may occur. The presented data refers to the final test run prior to the Microtransat competition in France [12], where the wind conditions have been within the operation range of the demonstration boat. The wind data during the 20-minute course are plotted in Fig. 14.

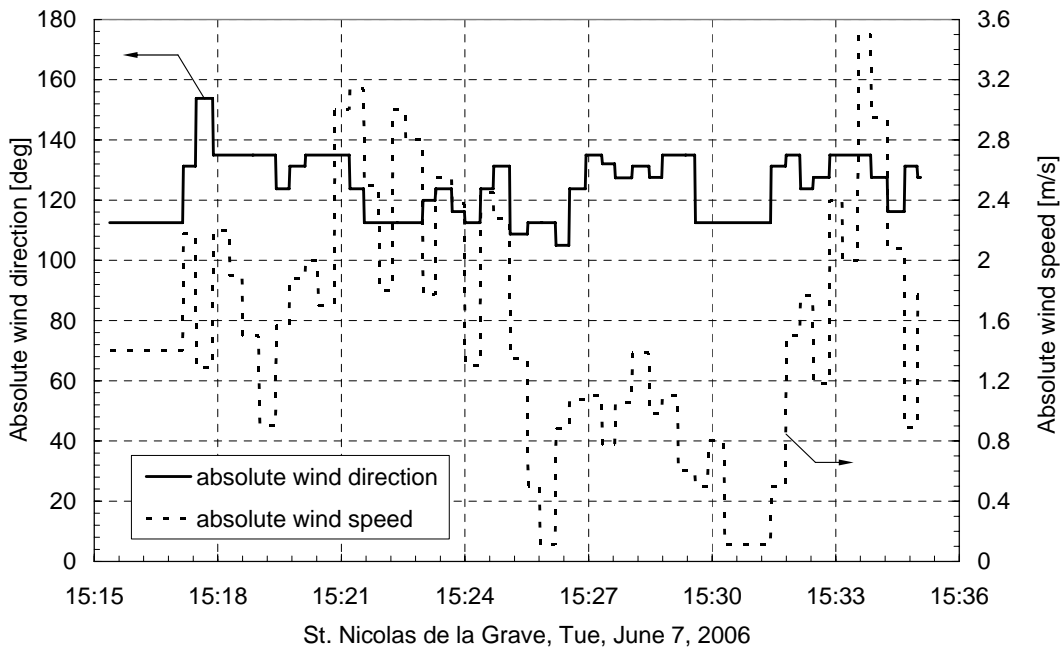


Fig. 14. Wind Log Data from the Test Run

Fig. 15 shows the GPS log data from the test run, where the task was to sail from Buoy 1 to Buoy 2 and back to Buoy 1. The boat polar diagram according to Table 1 has been applied for the routing algorithm and the beating parameter has been set to 60 m. It can be observed how the boat enters a beating band before reaching Buoy 2. The experiment is compared to simulation results using the varying measured wind data as an input. The dotted line is the result of a simulation where the boat model behaves strictly according

to the boat polar diagram. In reality, the boat behaviour is characterised by lateral displacement in the wind direction (leeway drift, Fig. 5). The dimensionless leeway factor f_d in Eq. (7) can be determined by graphical comparison between simulation and experimental data. The broken line in Fig. 15 shows the good agreement between the actual data and the simulation for a leeway factor of 0.1. The behaviour of the demonstration sail boat can therefore be described well by the assumed polar diagram (Eq. (9), Table 1, re-scaled by multiplication with a factor of 1.21) in combination with the leeway correction (Eq. (7), $f_d = 0.1$).

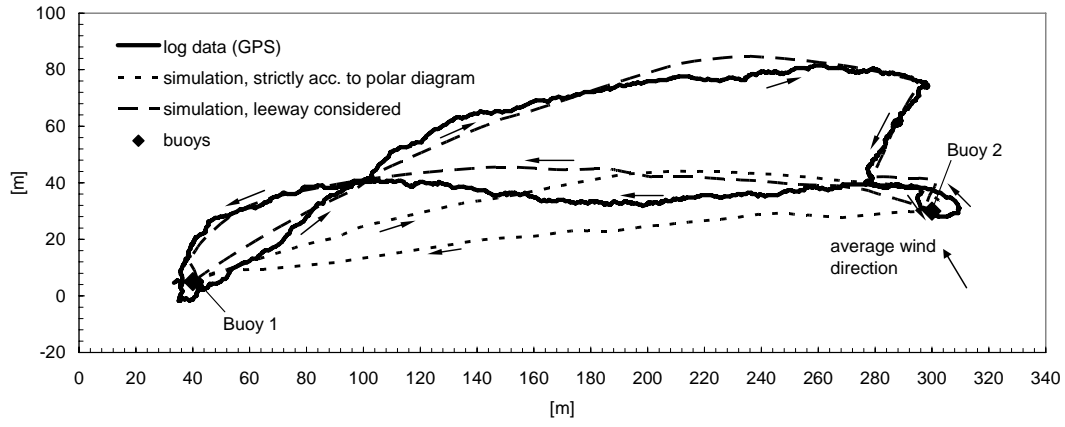


Fig. 15. Actual Run and Comparison to Simulation Results Based on Real Wind Data

Finally, the application of the simple polar diagram in the routing algorithm is tested and compared to the version using the boat polar diagram. The boat model behaves according to the boat polar diagram featuring the leeway correction. Fig. 16 shows that the algorithm featuring the simple polar diagram would have lead to a shorter route. The total time effort for the course is decreased by about 9 % (Table 3).

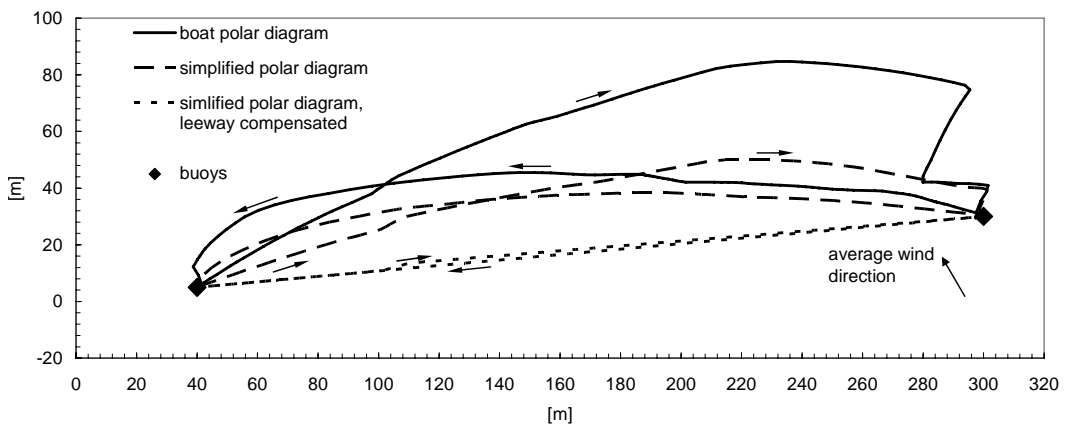


Fig. 16. Comparison of Algorithms Featuring either Boat Polar Diagram or Simple Polar Diagram

An additional simulation run has been carried out, where leeway is compensated inside the routing algorithm according to Eq. (7) and Fig. 5. This means, the boat always steers in direction $\vec{v}_b - \vec{v}_d$. Due to leeway drift, the actual movement of the boat changes to \vec{v}_b which is the desired direction of movement originally proposed by the routing algorithm. For the actual wind conditions of the experiment the leeway compensated simulation delivers the third route shown in Fig. 16 (dotted line). In this case the runtime further decreases. The deviation from the straight line route about two minutes after start is due to the temporary change in wind direction at this point (Fig. 14).

Route	Time Effort in s
Boat Polar Diagram	1135
Simple Polar Diagram	1035
Simple Polar Diagram; Leeway Compensated	970

Table 3

Runtime Comparison for Route in Fig. 16

Summarising the results, it can be stated that the algorithm finds suitable routes for real wind data also and that, again, a better route is found if the routing algorithm uses the simplified polar diagram instead of the actual boat polar diagram.

5 Conclusions

Autonomous sailboat navigation in real world conditions can be implemented in a first approach with the aim of imitating the behaviour of a human sailor. In the present work, a technique is presented to determine suitable boat headings in order to reach any target. The method works without knowledge of future weather conditions. This is advantageous especially for short term routing, where no accurate weather forecasts are available. The method is simple and easy to implement even on an embedded system. A parameter defines the width of a potential beating area. This beating parameter can be used to assure the boat to stay within a save area.

Simulations have shown that the routing strategy does not rely on the knowledge of the specific boat behaviour (polar speed diagram). The velocity made good is an important variable to be globally optimised within the routing strategy. However, it can be shown that simply maximising the velocity made good continuously does lead to sub-optimal results. The best results are obtained with a simplified polar diagram, which only defines the efficiently navigable range in terms of angles between boat and wind. The simplified polar diagram forces the boat to take the direct straight route even in situations

where the boat polar diagram proposes a different direction that is currently better but leads to a worse overall performance.

The parameters needed for the calculation of the desired boat heading are:

- target position
- current boat position
- current boat heading
- true wind direction

Tests of the method on an autonomous sailboat show its strength in dealing with a highly dynamic environment. The algorithm reacts in real-time on changing wind, like a sailor does.

The characteristic behaviour of the demonstration boat has been determined. By comparison between an experimental run and computer simulation the boat specific relationship between wind, boat velocity, and leeway has been determined. If leeway is considered in the computer model of the sail boat, the actual data log from the experiment and the simulated course match well.

The routing strategy does not consider yet obstacles like land masses or extreme weather phenomena. These aspects can potentially be incorporated in a combination with long-term routing methods.

Future work should therefore focus on:

- combination with long-term routing methods
- automatic dynamic determination of simple polar diagram
- automatic dynamic determination of the leeway factor
- automatic dynamic determination of optimal beating band width

The algorithm is expected to work independently of boat size. Short term goal is to implement it on a larger sailboat in order to succeed in the next Microtransat challenge. The competitors will have to demonstrate completely autonomous sailing on open sea.

6 Acknowledgements

The work has been carried out accompanying the participation of the Roboat-team at the first Microtransat challenge in Toulouse/France. Thanks to Yves Brière, ENSICA, Toulouse, for organising the competition and motivating this work. The authors also want to thank their team-colleagues Raphael Charwot (high-level programming, visualisation), Adrian Dabrowski (boat-shore communication), Karim Jafarmadar (boat and sensor implementation), Ira Lee

Kuhn (sailing skills), Matthias Hofmann (boat implementation), and Christian Löffler (mathematics) who all sacrificed spare time and private resources for the success of the project. The authors further acknowledge the scientific advice of Prof. Robert John, De Montfort University, Leicester.

A Nautical Terms

Apparent wind - The velocity of air as measured from a moving object, as a ship.

Beating (beat) - To sail towards the wind by making a series of tacks.

Great circle route - The shortest route between two points on the surface of a sphere, e.g. the earth.

Jib (jibe, gybe) - A jib, jibe or gybe is when a sailing boat turns its stern through the wind, such that the direction of the wind changes from one side of the boat to the other.

Leeway - The amount or angle of the drift of a ship to leeward from its heading.

Tack - A tack or coming about is the manoeuvre by which a sailing boat or yacht turns its bow through the wind so that the wind changes from one side to the other.

True wind - The velocity of air as measured from a platform fixed to the ground, such as an anchored boat.

Velocity made good - The speed of a yacht relative to the waypoint it wants to reach.

Windward - The side toward the wind.

References

- [1] J. A. Spaans, Windship routeing, *Journal of Windship Engineering and Industrial Aerodynamics* 19 (1985) 215–250.
- [2] R. H. Motte, R. S. Burns, S. Calvert, An overview of current methods used in weather routeing, *Journal of Navigation* 41 (1988) 101–114.
- [3] R. Stelzer, T. Proell, R. I. John, Fuzzy logic control system for autonomous sailboats, in: *Proceedings of IEEE International Conference in Fuzzy Systems (FUZZ-IEEE 2007)*, 2007.
- [4] T. Thornton, A review of weather routeing of sailboats, *Journal of Navigation* 46 (1993) 113–129.
- [5] J. A. Spaans, P. H. Stoter, New developments in ship weather routing 43 (1995) 95–106.

- [6] R. H. Motte, S. Calvert, On the selection of discrete grid systems of on-board micro-based weather routing, *Journal of Navigation* 1990 (1990) 104–117.
- [7] K. Stawicki, R. Smierzchalski, Methods of optimal ship routing for weather perturbations, in: *IFAC Conference on Control Applications in Marine System*, Glasgow, UK, 2001, pp. 101–106.
- [8] R. Smierzchalski, Z. Michalewicz, Modeling of ship trajectory in collision situations by an evolutionary algorithm, *IEEE Transactions on Evolutionary Computation* 4 (2000) 227–241.
- [9] R. Smierzchalski, Evolutionary-fuzzy system of safe ship steering in a collision situation at sea, in: *International Conference on Intelligent Agents, Web Technologies and Internet Commerce*, Vol. 1, 2005, pp. 893–898.
- [10] A. Philpott, A. Mason, Optimising yacht routes under uncertainty, in: *Proceedings of the 15th Chesapeake Sailing Yacht Symposium*, Annapolis, Maryland, 2001.
- [11] P. J. Richards, A. Johnson, A. Stanton, America’s cup downwind sails—vertical wings or horizontal parachutes?, *Journal of Wind Engineering and Industrial Aerodynamics* 89 (14-15) (2001) 1565–1577.
- [12] Y. Briere, First microtransat challenge, Available online: <http://www.ensica.fr/microtransat> (2006).